Distinct Differentiation Potential of Blood Monocyte Subsets in the Lung

Limor Landsman, Chen Varol and Steffen Jung

J Immunol 2007; 178:2000-2007; ;
http://www.jimmunol.org/content/178/4/2000

The Journal of Immunology is published twice each month by
The American Association of Immunologists, Inc.,
9650 Rockville Pike, Bethesda, MD 20814-3994.

Print ISSN: 0022-1767 Online ISSN: 1550-6606.

Distinct Differentiation Potential of Blood Monocyte Subsets in the Lung[1]

Limor Landsman, Chen Varol, and Steffen Jung[2]

Peripheral blood monocytes are a population of circulating mononuclear phagocytes that harbor potential to differentiate into macrophages and dendritic cells. As in humans, monocytes in the mouse comprise two phenotypically distinct subsets that are $Gr1^{high}CX_3CR1^{int}$ and $Gr1^{low}CX_3CR1^{high}$, respectively. The question remains whether these populations contribute differentially to the generation of peripheral mononuclear phagocytes. In this study, we track the fate of adoptively transferred, fractionated monocyte subsets in the lung of recipient mice. We show that under inflammatory and noninflammatory conditions, both monocyte subsets give rise to pulmonary dendritic cells. In contrast, under the conditions studied, only $Gr1^{low}CX_3CR1^{high}$ monocytes, but not $Gr1^{high}CX_3CR1^{int}$ cells, had the potential to differentiate into lung macrophages. However, $Gr1^{high}CX_3CR1^{int}$ monocytes could acquire this potential upon conversion into $Gr1^{low}CX_3CR1^{high}$ cells. Our results therefore indicate an intrinsic dichotomy in the differentiation potential of the two main blood monocyte subsets. ***The Journal of Immunology,*** **2007, 178: 2000–2007.**

Blood monocytes are considered circulating precursors of macrophages (MΦ)[3] and dendritic cells (DC) and, together with the latter, have collectively been termed mononuclear phagocytes (1, 2). Accordingly, when cultured in vitro in the presence of the cytokines M-CSF or GM-CSF, monocytes can be driven to differentiate into MΦ and DC, respectively (3, 4). Furthermore, in vivo studies also provide evidence that blood monocytes can act as precursors of MΦ (1, 5, 6). More recent reports have shown that monocytes can under inflammatory conditions differentiate in vivo into conventional $CD11c^{high}$ DC (cDC) (7, 8) and Langerhans cells (9). However, interestingly, blood monocytes seem not to contribute to the generation of splenic cDC (10–12).

Monocytes are, however, not a homogeneous cell population, but rather comprise at least two discrete subsets. Human monocytes consist of a $CD14^{2+}CD16^{-}$ population, which is $CCR2^{+}CD62L^{+}CX_3CR1^{int}$, and a $CD14^{+}CD16^{+}$ subset, which can be further characterized as being $CX_3CR1^{high}CCR2^{-}CD62L^{-}$ (8, 13, 14). In vitro culture and expression analysis of the human monocyte subsets suggest a particular role of $CD14^{+}CD16^{+}$ monocytes in inflammatory settings (15). More recently, monocyte dichotomy has also been established in mice and rats (8, 16, 17). Circulating murine $CD115^{+}$ monocytes encompass two main $Gr1^{high}CX_3CR1^{int}$ and $Gr1^{low}CX_3CR1^{high}$ subsets (8, 16), which based on their chemokine receptor expression correlate to human $CD14^{+/+}CD16^{-}$ and $CD14^{+}CD16^{+}$ monocytes, respectively (2, 8). Results of adoptive transfers of fractionated murine monocytes suggest that these cells are also functionally distinct: $Gr1^{low}$ monocytes were found to be recruited to resting tissues, whereas the $Gr1^{high}$ monocytes shuttle between the blood and the bone marrow (BM) unless recruited to sites of inflammation (8, 12). With regard to their differential fates, $Gr1^{high}$ monocytes were shown in mice to differentiate into cDC and Langerhans cells under inflammation (8, 9), and both $Gr1^{high}$ and $Gr1^{low}$ rat monocytes were reported to give rise to intestinal DC in steady state (17). However, for neither of the subsets the in vivo potential to become MΦ has been investigated. Furthermore, monocyte fate studies are complicated by the recent finding that $Gr1^{high}$ monocytes can convert in vivo into $Gr1^{low}$ monocytes (12, 18, 19). In addition, a comprehensive evaluation of the in vivo differentiation potential of monocytes has to consider that the monocyte fate is likely to be dictated by the tissue environment encountered upon their extravasation. Comparison of the differentiation potential of $Gr1^{high}$ and $Gr1^{low}$ monocytes therefore requires that the two subsets will be exposed to the same microenvironment and studied side by side.

Lymphoid and nonlymphoid organs often harbor tissue-specific mononuclear phagocyte members. In this study, we investigate the differentiation potential of adoptively transferred fractionated blood monocyte subsets into DC and MΦ, focusing on the pulmonary mononuclear phagocyte system as a nonlymphoid tissue model. The lung hosts well-defined MΦ and DC populations, which are believed to play opposing roles in the initiation and maintenance of lung inflammations (20–22). Importantly, expression of the β integrin CD11c discriminates both of these cell types from undifferentiated $CD11c^{-}$ monocytes found in this tissue (21, 23). Collectively, the pulmonary mononuclear phagocyte system is therefore particularly suited for a comparative monocyte differentiation study into either DC or MΦ.

In this study, we show that under both inflammatory and noninflammatory conditions, $Gr1^{high}CX_3CR1^{int}$ and $Gr1^{low}CX_3CR1^{high}$ monocytes give rise to pulmonary DC. In contrast, only $Gr1^{low}$, but not $Gr1^{high}$ monocytes harbor the immediate potential to differentiate into lung MΦ.

Department of Immunology, The Weizmann Institute of Science, Rehovot, Israel

Received for publication August 29, 2006. Accepted for publication December 1, 2006.

The costs of publication of this article were defrayed in part by the payment of page charges. This article must therefore be hereby marked *advertisement* in accordance with 18 U.S.C. Section 1734 solely to indicate this fact.

[1] This study was supported by the Minerva and the Pasteur-Weizmann Foundations. S.J. is the incumbent of the Pauline Recanati Career Development Chair and a scholar of the Benoziyo Center for Molecular Medicine.

[2] Address correspondence and reprint requests to Dr. Steffen Jung, Department of Immunology, The Weizmann Institute of Science, Rehovot 76100, Israel. E-mail address: s.jung@weizmann.ac.il

[3] Abbreviations used in this paper: MΦ, macrophage; DC, dendritic cell; BAL, bronchoalveolar lavage; BM, bone marrow; cDC, conventional $CD11c^{high}$ DC; DTx, diphtheria toxin; DTR, DTx receptor; FKN, fractalkine; int, intermediate; i.t., intratracheal; LN, lymph node; wt, wild type.

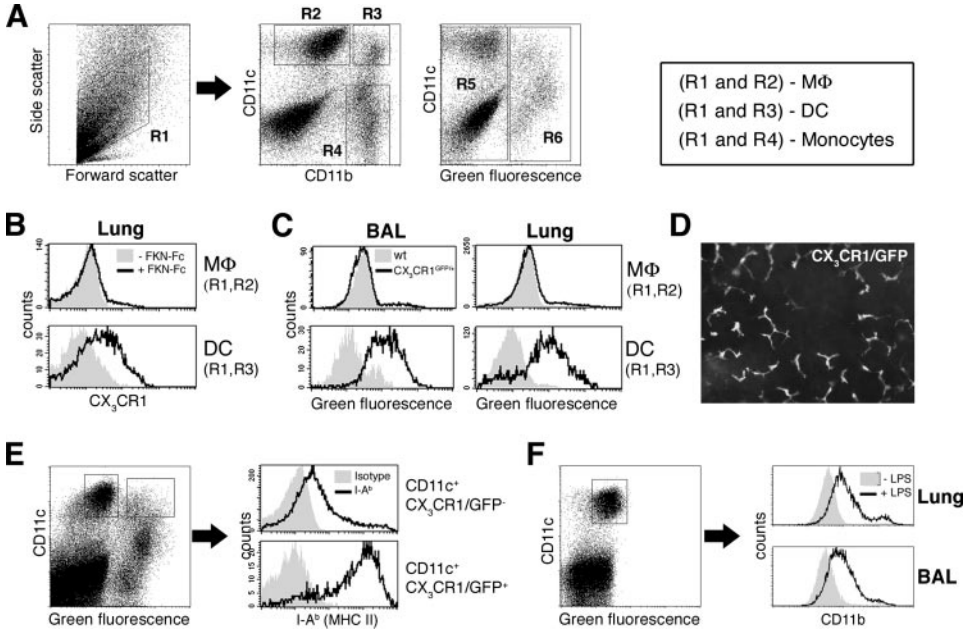

FIGURE 1. CX_3CR1/GFP expression by lung and alveolar mononuclear phagocytes. *A*, Flow cytometric analysis of lung cells of $cx_3cr1^{gfp/+}$ mouse. Cells were isolated and analyzed for expression of CD11c, CD11b, and green fluorescence. *Left panel*, Forward/side light scatter gate for living cells (R1). *Middle dot plot*, CD11c/CD11b expression pattern of cells of R1 gate and mononuclear phagocyte gates used in this study: $CD11c^+CD11b^-$ (R2, MΦ), $CD11c^+CD11b^+$ (R3, DC), and $CD11c^-CD11b^+$ (R4, monocytes) cells. *Right dot plot*, GFP expression of cells gated in R1 region and position of R5 (CX_3CR1/GFP negative) and R6 (CX_3CR1/GFP positive). Abs used were PE-coupled anti-CD11c and PerCP-conjugated anti-CD11b. *B*, FACS analysis of CX_3CR1 expression by lung MΦ (*upper panel*) and DC (*lower panel*) of $cx_3cr1^{gfp/+}$ mouse. Cells were either stained with Fc-coupled CX_3CR1 ligand (FKN-Fc), followed by Cy5-conjugated anti-Fc (+FKN-Fc, empty histogram), or with Cy5-conjugated anti-Fc alone (−FKN-Fc, gray filled histogram), followed by PE- and PerCP-coupled Abs against CD11c and CD11b, respectively. DC and MΦ were defined as cell gated in R1,R3 and R1,R2, respectively (as shown in *A*). *C*, FACS analysis of CX_3CR1/GFP expression by pulmonary MΦ and DC. Cells isolated from either BAL (*left panels*) or lungs (*right panels*) of $cx_3cr1^{gfp/+}$ (empty histogram) and wt (gray filled histogram) mice were analyzed for their green fluorescence intensity. DC and MΦ were defined as cells gated in (R1 and R3) and (R1 and R2), respectively (as shown in *A*). *D*, Live imaging of $cx_3cr1^{gfp/+}$;$rag1^{-/-}$ mouse lung by fluorescent microscopy showing GFP-labeled cells with DC morphology. *E*, FACS analysis of MHC class II ($I\text{-}A^b$) expression by $CD11c^+CX_3CR1/GFP^-$ (MΦ) and $CD11c^+CX_3CR1/GFP^+$ cells (DC) (*upper* and *lower panels*, respectively). Cells were isolated from a lung of $cx_3cr1^{gfp/+}$ mouse, and stained with either anti $I\text{-}A^b$ Ab (empty histograms) or isotype control (gray filled histograms). Histograms show cells gated, as indicated in dot plot. *F*, CD11b expression by lung and alveolar MΦ of untreated and endotoxin-treated mice. Histograms show CD11b expression by $CD11c^+$ autofluorescent lung and BAL wt cells (MΦ) (gated as indicated in dot plot) of untreated (gray filled histograms) and LPS-treated (200 ng i.t. on day 1; empty histograms) wt mice.

Materials and Methods

Mice

This study involved the use of the C57BL/6 mouse strains *CD11c*: Diphtheria toxin (DTx) receptor (DTR) transgenic mice (B6.FVB-Tg(Itgax-DTR/GFP)57Lan/J; The Jackson Laboratory) that carry a human DTR transgene under the murine CD11c promotor (24); CX_3CR1^{GFP} mice harboring a targeted replacement of the cx_3cr1 gene by a GFP reporter (25); $rag1^{-/-}$ mice (B6.129S7-*Rag1tm1Mom*/J; The Jackson Laboratory) that lack mature lymphocytes; $cd80^{-/-}/cd86^{-/-}$ mice (B6.129S4-$Cd80^{tm1Shr}Cd86^{tm1Shr}$/J; The Jackson Laboratory) that lack expression of both CD80 and CD86 costimulatory molecules (26); and OT-II TCR transgenic mice (C57BL/6-Tg(TcraTcrb)425Cbn/J; The Jackson Laboratory) harboring $CD4^+$ T cells specific for OVA (27, 28). Animals were backcrossed to mice bearing the CD45.1 allotype (B6.SJL-$Ptprc^a$ $Pepc^b$/BoyJ; The Jackson Laboratory), when indicated. The wild-type (wt) C57BL/6 mice were purchased from Harlan Teklad. All mice were maintained under specific pathogen-free conditions and handled under protocols approved by the Weizmann Institute Animal Care Committee according to international guidelines.

Cell isolations

Mice were sacrificed, and blood was collected from the main artery. For bronchoalveolar lavage (BAL), the trachea was exposed to allow insertion of a catheter, through which the lung was filled and washed four times with 1 ml of PBS without Ca^{2+}/Mg^{2+}. Lung parenchyma and spleens were then collected, and tissues were digested with either 4 mg/ml (lung) or 1 mg/ml (spleen) collagenase D (Roche) for 1 h at 37°C, followed by incubation with ACK buffer to lyse erythrocytes. Following their isolation, mediastinal lymph nodes (LNs) were passed through a mesh and cells were collected. All isolated cells were suspended in PBS supplemented with 2 mM EDTA, 0.05% sodium azide, and 1% FCS.

Flow cytometric analysis

The following fluorochrome-labeled mAbs were purchased from BD Pharmingen or eBioscience and used according to manufacturers' protocols: PE-conjugated anti-CD11c, $I\text{-}A^b$, and CD115 Abs; allophycocyanin-conjugated anti-CD11c, CD11b, CD4, and Gr1 (Ly6C/G) Abs; PerCP-conjugated anti-CD11b Ab; biotin-conjugated anti-CD45.1 Ab; and allophycocyanin- and PE-conjugated streptavidin. CX_3CR1 staining using the CX_3CR1 ligand fractalkine (FKN) was performed, as previously described (25). Briefly, cells were incubated with a FKN-Fc fusion protein (provided by Millenium Biotherapeutics) or PBS, followed by incubation with Cy5-conjugated anti-human Fc Ab. After an intensive wash, cells were incubated with indicated Abs. Cells were analyzed on a FACSCalibur cytometer (BD Biosciences) using CellQuest software (BD Biosciences).

Cell transfers

For blood monocyte transfers, ~20 mice were sacrificed and blood was collected to obtain an average of 15 ml of blood for each experiment. Erythrocytes and neutrophils were removed by a Ficoll density gradient (Amersham). Cells were washed and exposed to biotin-conjugated anti-CD115 or anti-Gr1 Abs (eBioscience), followed by incubation with streptavidin-conjugated MACS beads (Miltenyi Biotec). Cells were then magnetically separated, according to manufacturer's protocol. Indicated fractions were collected and i.v. injected to recipient mice. For BM monocyte transfers, cells were isolated from donor femora and tibiae and enriched for mononuclear cells on a Ficoll density gradient, followed by immunostaining with PE-conjugated anti-CD115 and allophycocyanin-conjugated

anti-Gr1 Abs (eBioscience). BM monocytes were then purified by high speed sorting using FACSAria (BD Biosciences). For T cell transfers, $CD4^+$ T cells were isolated from OT-II;CD45.1 mice by enrichment using CD4-conjugated MACS beads (Miltenyi Biotec), according to manufacturer's protocol.

Intratracheal (i.t.) instillation

PBS (80 μl) containing either DTx (catalog 150; List Biological Laboratories), LPS (*Escherichia coli* 055:B5; Sigma-Aldrich catalog L4005), or OVA (Sigma-Aldrich; catalog A5503) was applied to mouse tracheae, as previously described, with modifications (29). Briefly, mice were lightly anesthetized using isoflurane and placed vertically, and their tongues were pulled out. Using a long-nasal tip, liquid was placed at trachea top and actively aspirated by the mouse. Gasping of treated mice verified liquid application to the alveolar space.

Microscopy of lung parenchyma

Lungs were filled with 2% low melting agarose (Sigma-Aldrich; catalog A0701), as previously described (30). Live tissues were cut and imaged with a Zeiss Axioskop II fluorescent microscope using Simple PCI software.

Results

CX_3CR1 expression discriminates between pulmonary MΦ and DC

Alveolar and lung MΦ and DC have been defined according to discrete surface marker expression. Both MΦ and DC express the β integrin CD11c, whereas DC are further characterized as $CD11b^+$ cells, and MΦ are $CD11b^-$ (21, 23, 31) (Fig. 1*A*). In addition, lung and alveolar MΦ, but not DC, are autofluorescent (31, 32). In this study, we show that lung MΦ and DC also differ in their expression of the chemokine receptor CX_3CR1. Thus, surface staining with an Fc fusion of the CX_3CR1 ligand FKN/CX_3CL1 (FKN-Fc) showed that $CD11c^+CD11b^+$ lung DC are CX_3CR1 positive, whereas $CD11c^+CD11b^-$ MΦ are CX_3CR1 negative (Fig. 1*B*). Accordingly, in CX_3CR1^{GFP} knockin mice, whose *cx_3cr1* gene was replaced by a GFP cassette (25), lung and BAL DC express GFP (Fig. 1, *C* and *D*), whereas lung and BAL MΦ do not (Fig. 1*C*).

Lung DC can be further characterized as $CD11c^+$MHC-II^{high} cells, whereas lung MΦ are $CD11c^+$MHC-II^{low} (21, 31). Staining for MHC-II revealed that $CD11c^+CX_3CR1/GFP^+$ cells also express high levels of MHC-II, whereas $CD11c^+CX_3CR1/GFP^-$ cells are MHC-II^{low} (Fig. 1*E*), supporting their definition as DC and MΦ, respectively (31). Interestingly, we recently reported the same CX_3CR1 expression pattern for small intestinal lamina propria DC and MΦ (33). CX_3CR1 is therefore a reliable marker allowing discrimination of $CD11c^+$ DC and MΦ in the lung and alveolar space. In contrast, we have observed that CD11b expression is significantly up-regulated on lung and alveolar MΦ under inflammation (Fig. 1*F*).

For the remainder of this study that investigates the differential origin of pulmonary MΦ and DC, we therefore apply a stringent definition of the two cell types by considering $CD11c^+CD11b^+$ CX_3CR1/GFP^+ cells (Fig 1*A*; R1, R3, and R6 gated cells) as lung DC, and $CD11c^+CD11b^-CX_3CR1/GFP^-$ (Fig 1*A*; R1, R2, and R5 gated cells) as resting lung MΦ. Monocytes found in the lung parenchyma have previously been characterized as $CD11c^-$ $CD11b^+$ cells and are defined accordingly (23) (Fig. 1*A*; gates R1 and R4).

Blood monocytes can differentiate into lung DC in naive mice

The most direct way to study the fate of blood monocytes is arguably the adoptive transfer of these cells into recipient's bloodstream and subsequent tracking of graft descendants. To study the monocyte differentiation potential, we isolated the cells from donor blood according to surface expression of the monocyte-specific marker CD115 (M-CSF-R) using magnetic separation. Notably,

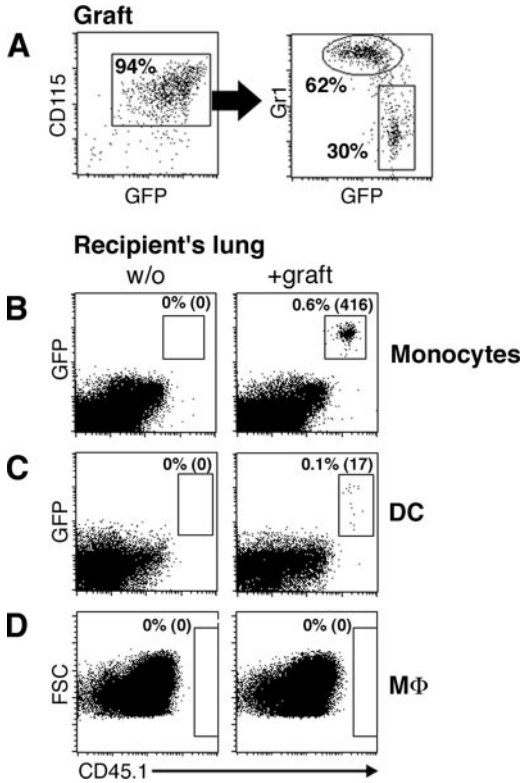

FIGURE 2. Grafted peripheral blood monocytes give rise to lung DC, but not MΦ in untreated recipient mice. *A*, FACS analysis of representative MACS-enriched $CD115^+$ cell graft isolated from *$cx_3cr1^{gfp/+}$*;CD45.1 donor blood. Note presence of $Gr1^{high}CX_3CR1/GFP^{int}$ and $Gr1^{low}CX_3CR1/GFP^{high}$ monocyte subsets. *B–D*, Lungs of untreated monocyte recipients, day 4 after transfer. CD45.2 wt recipients either received CX_3CR1/GFP^+ CD45.1 blood $CD115^+$ graft (10^6 cells, +graft) or no graft (w/o) on day 0. Lung monocytes (*B*, $CD11c^-CD11b^+$ cells gated according to Fig. 1*A* (R1 and R4)), DC (*C*, $CD11c^+CD11b^+$ cells gated according to Fig. 1*A* (R1 and R3)), and MΦ (*D*, $CD11c^+CD11b^-CX_3CR1/GFP^-$ cells gated according to Fig. 1*A* (R1, R2, and R5)) were analyzed on day 4 for graft-derived cells. Numbers indicate percentage of graft-derived cells ($CX_3CR1/GFP^+CD45.1^+$ or $CD45.1^+$) of total gated population and their absolute numbers (in parentheses). Data show one representative of three independent experiments involving one to two recipients per group.

this cell population included $Gr1^{high}$ and $Gr1^{low}$ monocyte subsets (Fig. 2*A*), both of which express CX_3CR1 (8). To distinguish between graft- and host-derived cells, donor monocytes were retrieved from blood of *$cx_3cr1^{gfp/+}$*;CD45.1 mice and transferred into congenic CD45.2 wt recipients. Graft-derived lung DC are therefore CD45.1 CX_3CR1/GFP positive (Fig. 1*C*), whereas host DC are CD45.1 GFP negative. The identification of graft-derived CX_3CR1/GFP-negative MΦ in recipient lungs relies solely on expression of the allotypic CD45 marker: whereas graft-derived MΦ will be CD45.1, host cells are CD45.2. Successful monocyte transfers were confirmed by detection of grafted monocytes in the recipients' lungs (Figs. 2*B* and 4*A*), blood, and spleens (data not shown).

We first transferred monocytes to untreated wt recipient mice, and analyzed their lung and alveolar space content 4 days later. We detected graft-derived cells in recipient's lung, most of which were undifferentiated $CD11c^-CD11b^+CX_3CR1/GFP^+$ monocytes (Fig. 2*B*). We also consistently observed few GFP-expressing $CD11c^+$ $CD11b^+$ lung DC (Fig. 2*C*), indicating differentiation of monocytes into DC in steady state. Despite the fact that MΦ outnumber DC by far in this tissue, we did, however, not detect donor-derived ($CD45.1^+$) lung MΦ (Fig. 2*D*). In addition, we could not detect graft-derived cells in recipients' alveolar space (data not shown).

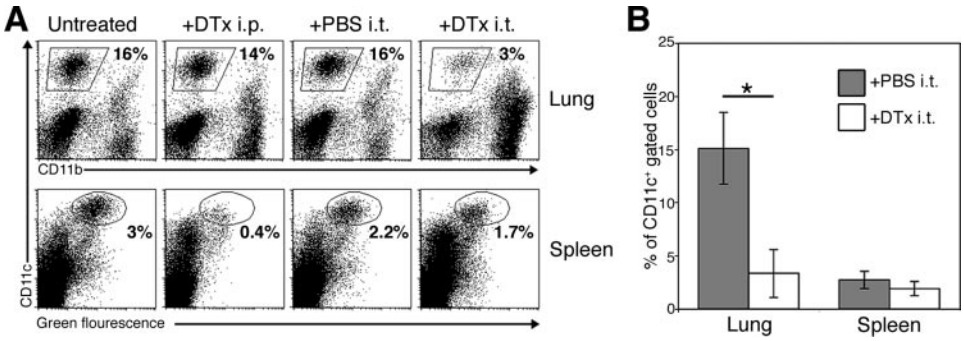

FIGURE 3. In vivo depletion of lung *CD11c*:DTR transgenic CD11c$^+$ cells, but not splenic CD11c$^+$ cells, upon i.t. instillation of DTx. *CD11c*:DTR mice were treated with DTx either i.p. (4 ng/gr, +DTx i.p.) or i.t. (100 ng, +DTx i.t.). Control littermates were either treated with PBS i.t. (+PBS i.t.) or left untreated. Lungs and spleens were analyzed 1 day after treatments. *A*, FACS analysis of lung cells for CD11c and CD11b expression (*upper panels*) and spleen cells for CD11c$^+$ and GFP expression (*lower panels*). Numbers indicate percentage of gated cells from total cells. *B*, Bar diagram summarizing percentages of CD11c$^+$ spleen and lung cells (gated as in *A*) of mice treated i.t. with either DTx (100 ng) or PBS. Mice were analyzed 1 day after treatments. $n = 4$. $*$, $p < 0.005$ (two-tailed Student's t test).

Blood monocytes can differentiate into lung DC and MΦ in mononuclear phagocyte-depleted mouse

The failure to detect graft-derived lung MΦ in untreated recipients could indicate that those cells do not originate from CD115$^+$ blood monocytes. Alternatively, the long-lived respiratory MΦ compartment might in steady state require only limited cellular input from the blood, which could be below our level of detection. To distinguish between these options, we decided to ablate lung MΦ before the monocyte transfer.

We took advantage of *CD11c*:DTR transgenic mice that allow the specific depletion of CD11c^{high} cells (24). The i.t. DTx instillation of *CD11c*:DTR transgenic mice results in the ablation of CD11c$^+$ lung mononuclear phagocytes, including DC and MΦ (34) (Fig. 3). Depletion of endogenous pulmonary MΦ by the DTx treatment of *CD11c*:DTR recipients might open otherwise closed niches to newly coming cells. Notably, in this strategy, grafted cells, which are not *CD11c*:DTR transgenic, are resistant to ablation.

We next transferred CX_3CR1^{GFP} CD45.1 monocytes to DTx-treated *CD11c*:DTR;CD45.2 recipients. Four days after transfer, recipient mice were analyzed by flow cytometry for the presence of graft-derived mononuclear phagocytes in their lung and alveolar space. We readily observed graft-derived parenchymal lung and alveolar CX_3CR1/GFP^+ DC in the recipient mice (Fig. 4, *B*, *D*, and *F*). Importantly, as opposed to the untreated recipients, we also could detect graft-derived CD45.1 MΦ in recipient's lung (Fig. 4*C*), suggesting that the ablation of endogenous lung MΦ promoted the seeding of the lung with graft-derived cells. Graft-derived monocytes, DC, and MΦ could also be detected upon perfusion of the recipients, indicating their location in the lung parenchyma (data not shown).

Taken together, these results show that adoptively transferred CD115$^+$ blood monocytes collectively have the capacity to differentiate into pulmonary DC and MΦ.

Monocyte-derived lung DC can prime naive T cells

DC are best defined by their unrivaled capacity to stimulate naive T cells (35, 36). Importantly, in the pulmonary mononuclear system, MΦ are established suppressors of T cell activation (20–22, 37). We therefore sought to study the functionality of graft-derived lung DC by transferring monocytes into mutant mice that lack the essential costimulatory molecules CD80 and CD86, and hence are incapable of naive T cell priming (26, 38).

We first tested the ability of grafted OVA-specific TCR transgenic T cells (OT-II) (27) to respond to i.t. OVA challenge in wt and *cd80*$^{-/-}$;*cd86*$^{-/-}$ recipient mice (Fig. 5*A*). Mice received an OT-II;CD45.1 CD4$^+$ T cell graft (day 0), followed by an i.t. challenge with OVA and LPS on the 3 subsequent days (days 1–3). Seven days after the initial immunization (day 8), mediastinal LNs were isolated and analyzed for the presence of OVA-specific

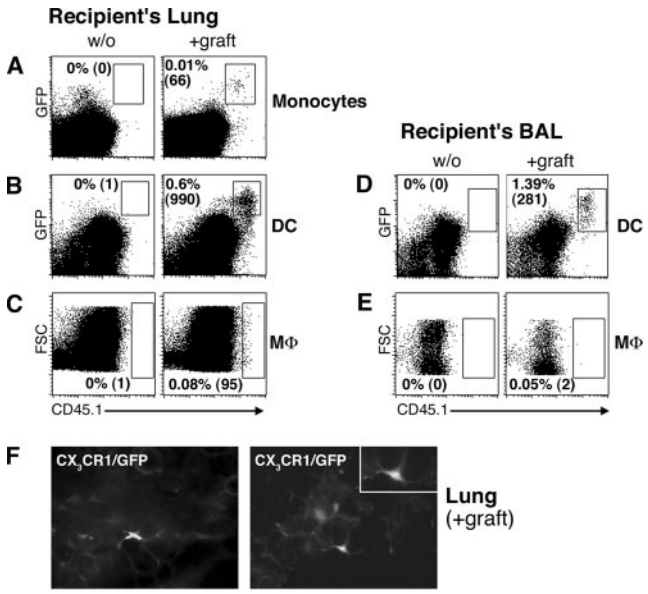

FIGURE 4. Grafted peripheral blood monocytes give rise to lung DC and MΦ in mononuclear phagocyte-depleted recipient mice. *A–E*, DTx-treated *CD11c*:DTR monocyte recipient lung, day 4 after transfer. *CD11c*:DTR;CD45.2 mice pretreated i.t. with DTx (100 ng, day 0) either received *cx*$_3$*cr1*$^{gfp/+}$;CD45.1 CD115$^+$ blood monocyte graft (10^6 cells, +graft) or no graft (w/o) 2 h after DTx treatment. Lung monocytes (*A*, CD11c$^-$CD11b$^+$ cells gated according to Fig. 1*A* (R1 and R4)), DC (*B*, CD11c$^+$CD11b$^+$ cells gated according to Fig. 1*A* (R1 and R3)), and MΦ (*C*, CD11c$^+$CD11b$^-$CX$_3$CR1/GFP$^-$ cells gated according to Fig. 1*A* (R1, R2, and R5)), as well as BAL DC (*D*, CD11c$^+$ CD11b$^+$ cells gated according to Fig. 1*A* (R1 and R3) and MΦ (*E*, CD11c$^+$CD11b$^-$CX$_3$CR1/GFP$^-$ cells gated according to Fig. 1*A* (R1, R2, and R5)) were analyzed on day 4 for graft-derived cells. Numbers indicate percentage of graft-derived cells (CX$_3$CR1/GFP$^+$CD45.1$^+$ or CD45.1$^+$) of total population and their absolute numbers (in parentheses). Data show representative results of three independent experiments involving one to two mice per group. *F*, Histological analysis of DTx-treated monocyte recipient lung. *CD11c*:DTR mouse was treated with DTx i.t. (100 ng, day 0) and received CX_3CR1^{GFP} blood monocyte graft 2 h later, as previously described. Pictures show green fluorescent cells with DC morphology in different areas of recipient lung.

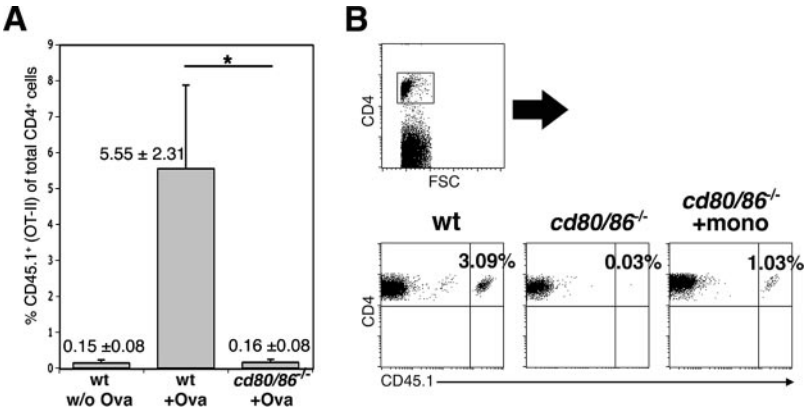

FIGURE 5. Rescue of *CD80/CD86* knockout phenotype by monocyte-derived APC. *A*, Impaired anti-OVA response of adoptively transferred OT-II CD4$^+$ T cells in mice lacking CD80 and CD86 molecules. The wt (CD45.2) and *cd80*$^{-/-}$;*cd86*$^{-/-}$ (CD45.2) mice received an OT-II;CD45.1 OVA-specific T cell graft (10^6 cells) on day 0. Recipients were treated i.t. with either 10 μg of OVA and 100 ng of LPS (wt + Ova, *cd80/86*$^{-/-}$ + Ova) or LPS alone (wt w/o Ova) on days 1, 2, and 3. Mediastinal LNs were isolated on day 8 and analyzed for the presence of CD45.1$^+$ grafted T cells. Bar diagram shows percentage of CD45.1$^+$CD4$^+$ cells of the total CD4$^+$ T cell population (group size: $n = 5$ for OVA-treated groups, and $n = 3$ for LPS-treated group). Numbers indicate percentage of CD45.1$^+$ cells of total CD4$^+$ cells, followed by the appropriate SDs. $*$, $p < 0.01$ (two-tailed Student's t test). *B*, Monocyte transfer reconstitutes priming of OVA-specific CD4 T cells in *cd80*$^{-/-}$;*cd86*$^{-/-}$ mice. The wt and *cd80*$^{-/-}$;*cd86*$^{-/-}$ mice received OT-II grafts on day 0, as described in *A*. One day later, *cd80*$^{-/-}$;*cd86*$^{-/-}$ mice also received either *cx*$_3$*cr1*$^{+/GFP}$;*rag1*$^{-/-}$;CD45.2 CD115$^+$ blood monocyte graft (5×10^5 cells, *cd80/86*$^{-/-}$ +mono) or no graft (*cd80/86*$^{-/-}$). Three hours before monocyte transfer and on days 2 and 3, all mice were i.t. treated with OVA (10 μg) and LPS (100 ng), as described in *A*. Mediastinal LNs were collected on day 8, and the percentage of CD45.1$^+$ cells of total CD4$^+$ T cells was determined for each mouse. Data show one representative of three independent experiments involving one to two mice per group.

CD4$^+$ T cells (CD45.1$^+$). The levels of surviving grafted T cells in OVA/LPS-challenged *cd80*$^{-/-}$;*cd86*$^{-/-}$ recipients were significantly lower than in OVA/LPS-challenged wt recipients and comparable to those of LPS-challenged control recipients (Fig. 5*A*). In conclusion, due to the absence of competent lung DC in these *cd80*$^{-/-}$:*cd86*$^{-/-}$ mice, grafted OVA-specific TCR transgenic

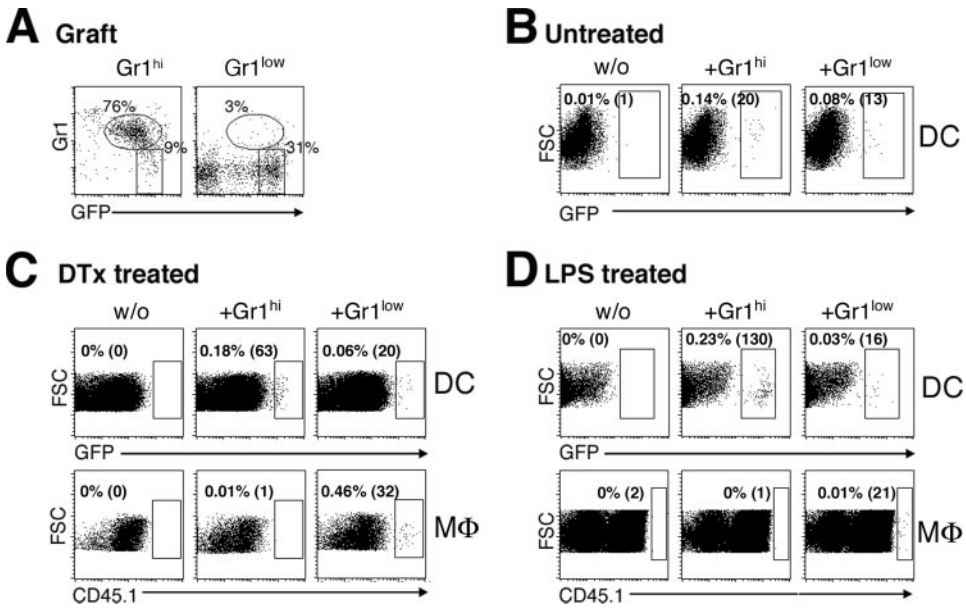

FIGURE 6. Distinct donor-derived mononuclear phagocyte populations in recipients of Gr1^{high} and Gr1^{low} monocyte grafts. *A*, FACS analysis of representative *cx*$_3$*cr1*$^{gfp/+}$;*rag1*$^{-/-}$;CD45.1 monocyte grafts, MACS fractionated according to Gr1 expression. Dot plots show isolated Gr1^{high}CX$_3$CR1/GFP^{int} (*left*) and Gr1^{low} CX$_3$CR1/GFP^{high} (*right*) blood monocytes. *B*, Untreated wt mice received Gr1^{high} (3×10^5 CX$_3$CR1/GFP^{int}Gr1^{high} cells), Gr1^{low} (3×10^5 CX$_3$CR1/GFP^{high}Gr1^{low} cells) grafts, or no graft on day 0, as described in *A*. Lung DC were analyzed on day 4 for graft-derived (CX$_3$CR1/GFP$^+$) cells. DC are defined as CD11c$^+$CD11b$^+$ cells gated according to Fig. 1*A* (R1 and R3). Data show one representative of three independent experiments involving one to two mice per group. *C*, DTx-treated *CD11c*:DTR;CD45.2 mice were pretreated i.t. with DTx (100 ng) and received Gr1^{high} (2.5×10^5 CX$_3$CR1/GFP^{int}Gr1^{high} cells) graft, Gr1^{low} (1×10^5 CX$_3$CR1/GFP^{high}Gr1^{low} cells) graft, or no graft on day 0. Lung DC and MΦ were analyzed on day 4 for graft-derived cells. DC are defined as CD11c$^+$CD11b$^+$ cells gated according to Fig. 1*A* (R1 and R3). MΦ are defined as CD11c$^+$CD11b$^-$CX$_3$CR1/GFP$^-$ cells gated according to Fig. 1*A* (R1, R2, and R5). Data are representative of three independent experiments involving one to two mice per group. *D*, The wt recipients (CD45.2) pretreated i.t. with LPS (200 ng) received Gr1^{high} (4×10^5 CX$_3$CR1/GFP^{int}Gr1^{high} cells), Gr1^{low} (2.5×10^5 CX$_3$CR1/GFP^{high}Gr1^{low} cells), or no graft on day 0. Lung DC and MΦ compartments (defined as CD11c$^+$CD11b$^+$ cells gated according to Fig. 1*A* (R1 and R3) and CD11c$^+$CD11b$^-$CX$_3$CR1/GFP$^-$ cells gated according to Fig. 1*A* (R1, R2, and R5), respectively) were analyzed on day 4 for graft-derived cells. Data are representative of three independent experiments involving one to two mice per group. Numbers in *B–D* indicate percentage of graft-derived gated cells (CX$_3$CR1/GFP$^+$ or CD45.1$^+$) of total indicated population and their absolute numbers (in parentheses).

$CD4^+$ T cells failed to respond to i.t. OVA challenge (Fig. 5*A*). We then tested the ability of wt blood monocytes to reconstitute OT-II $CD4^+$ T cell response in $cd80^{-/-}$:$cd86^{-/-}$ mice. One day after OT-II T cell transfer, $cd80^{-/-}$;$cd86^{-/-}$ mice either received a monocyte graft or no graft. To exclude B cell contaminations, $CD115^+$ blood monocytes were retrieved from $cx_3cr1^{gfp/+}$;$rag1^{-/-}$;CD45.2 mice, which lack mature lymphocytes. Three hours before monocyte transfer, and on the 2 following days, all mice were challenged i.t. with OVA and LPS. Seven days after the initial immunization, we isolated the mediastinal LNs and analyzed them for the presence and proliferative expansion of OVA-specific $CD4^+$ T cells ($CD45.1^+$). As seen in Fig. 5*B*, monocyte-derived DC partially reconstituted the OVA-specific $CD4^+$ T cell response. This in vivo rescue of the CD80/CD86 deficiency confirms that adoptively transferred monocytes differentiated in the recipients into bona fide lung DC that are capable of priming naive T cells.

$Gr1^{high}$ and $Gr1^{low}$ blood monocyte subsets differ in their potential to become either DC or MΦ

The adoptive transfer of blood monocytes established that this heterogeneous population includes cells that can differentiate into both lung DC and MΦ (Fig. 4). We next decided to test whether the two $Gr1^{high}CX_3CR1^{int}$ and $Gr1^{low}CX_3CR1^{high}$ monocyte subsets (8) differ in their potential to give rise to pulmonary mononuclear phagocytes. To this end, we fractionated blood of $cx_3cr1^{gfp/+}$;$rag1^{-/-}$;CD45.1 donor mice by magnetic separation according to Gr1 expression (Fig. 6*A*) and injected the monocyte fractions into CD45.2 recipients.

To study the differentiation potential of $Gr1^{high}$ and $Gr1^{low}$ blood monocytes in steady state, we first transferred them into untreated wt recipients and analyzed their lungs 4 days later. In agreement with our previous data (Fig. 2*B*), both subsets failed to give rise to lung MΦ under these conditions (data not shown). Graft-derived CX_3CR1/GFP^+ DC could be detected in recipients that had received either $Gr1^{high}$ or $Gr1^{low}$ blood monocytes (Fig. 6*B*). This indicates that in steady state both monocyte subsets reach the lung and can give rise to DC.

We next examined the monocyte subset fate in recipients depleted of endogenous mononuclear phagocytes. To this end, we transferred Gr1-fractionated CX_3CR1^{GFP} CD45.1 blood cells into *CD11c*:DTR CD45.2 recipients that were pretreated i.t. with DTx. Also, under these conditions, we were able to detect graft-derived DC in recipients of either of the subsets (Fig. 6*C*). Interestingly, however, $CD45.1^+$ graft-derived lung MΦ were only observed in recipients of the $Gr1^{low}$ monocyte graft, but not in the lungs of $Gr1^{high}$ monocyte recipients (Fig. 6*C*). This suggests that $Gr1^{low}$ blood monocytes, but not $Gr1^{high}$ monocytes, have the potential to give rise to lung MΦ under the conditions studied.

It was shown recently that endotoxin exposure accelerates replacement of pulmonary MΦ by BM-derived cells as compared with noninflammatory conditions (39). In the DTx-induced cell ablation system, targeted cells die by apoptosis (24, 40) and their replenishment might therefore mimic noninflammatory conditions. To investigate the differentiation potential of the monocyte subsets under inflammation, we therefore transferred Gr1-fractionated CX_3CR1^{GFP} donor blood into wt recipients (CD45.2) pretreated i.t. with LPS. Both $Gr1^{low}$ and $Gr1^{high}$ monocyte subsets readily gave rise to DC (Fig. 6*D*). However, again only in recipients of $Gr1^{low}$ monocytes, we detected graft-derived lung MΦ (Fig. 6*D*).

In summary, our adoptive cell transfer experiments suggest that under inflammatory and noninflammatory conditions, both $Gr1^{high}$ and $Gr1^{low}$ blood monocytes can give rise to lung DC. Importantly, in our experimental system, only $Gr1^{low}$ monocytes, but not the $Gr1^{high}$ cells, gave rise to lung MΦ.

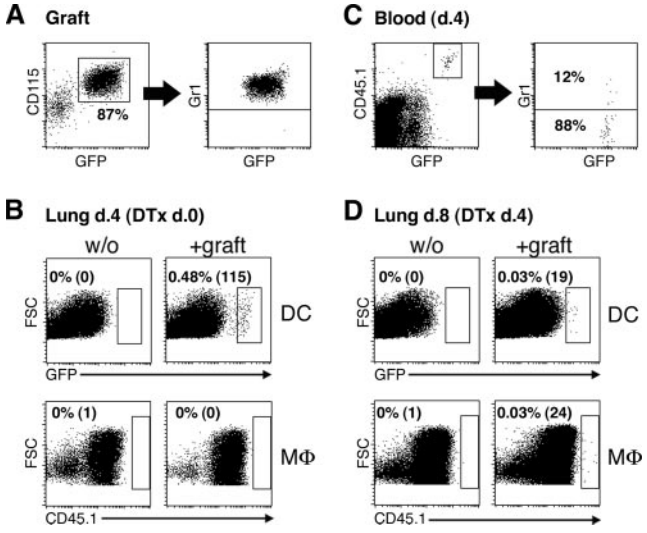

FIGURE 7. $Gr1^{high}$ monocytes give rise to lung MΦ after conversion into $Gr1^{low}$ monocytes. *A*, FACS analysis of $CD115^+CX_3CR1/GFP^{int}Gr1^{high}$ BM monocytes purified from $cx_3cr1^{gfp/+}$;CD45.1 mouse femora and tibiae using FACSAria cell sorter. *B* and *C*, *CD11c*:DTR mice pretreated i.t. with DTx (100 ng) received a $Gr1^{high}$ BM monocyte graft (10^6 cells) or no graft on day 0. *B*, Recipient lung MΦ and DC compartments (defined as $CD11c^+CD11b^+$ cells gated according to Fig. 1*A* (R1 and R3) and $CD11c^+CD11b^-CX_3CR1/GFP^-$ cells gated according to Fig. 1*A* (R1, R2, and R5), respectively) were analyzed on day 4 for graft-derived cells (CX_3CR1/GFP^+ or $CD45.1^+$). Numbers indicate percentage of gate cells of total indicated population and their absolute numbers (in parentheses). Data show one representative of three independent experiments involving one to two mice per group. *C*, Recipient blood was analyzed on day 4 for $CX_3CR1/GFP^+CD45.1^+$ graft-derived cells for Gr1 expression (*left panel*). Recovered population is equivalent to 10^3–10^4 total donor monocytes per recipient's bloodstream. *D*, *CD11c*:DTR recipients received a $Gr1^{high}$ monocyte graft (2×10^6 cells) or no graft on day 0, and were i.t. treated with DTx (100 ng) on day 4. Lung DC and MΦ (defined as $CD11c^+CD11b^+$ cells gated according to Fig. 1*A* (R1 and R3) and $CD11c^+CD11b^-CX_3CR1/GFP^-$ cells gated according to Fig. 1*A* (R1, R2, and R5), respectively) were analyzed on day 8 for graft-derived cells. Gates show and numbers indicate percentage of graft-derived cells (CX_3CR1/GFP^+ or $CD45.1^+$) of total population and their absolute numbers (in parentheses). Data show one representative of three independent experiments involving one to two mice per group.

Upon conversion into $Gr1^{low}$ monocytes, $Gr1^{high}$ BM monocytes gain the potential to generate lung MΦ

Recent studies have established that $Gr1^{high}$ monocytes are efficient precursors of $Gr1^{low}$ monocytes (12, 18, 19). This suggests that the failure of $Gr1^{high}$ blood monocytes to give rise to lung MΦ in our system (Fig. 6, *C* and *D*) might be due to the fact that the time window between transfer and analysis (4 days) was too short for both $Gr1^{high}/Gr1^{low}$ monocyte conversion and MΦ differentiation to occur.

To directly test whether grafted $Gr1^{high}$ monocytes can gain the ability to give rise to MΦ through a $Gr1^{low}$ monocyte intermediate, we investigated the ability of $Gr1^{high}$-derived $Gr1^{low}$ monocytes to give rise to lung MΦ. Isolation of cells from donor BM allows obtaining larger amounts of $Gr1^{high}$ monocyte as compared with the blood ($\sim 0.5 \times 10^6$ cells/femur vs $\sim 0.5 \times 10^5$ cells/ml blood). We therefore isolated cells from BM of $cx_3cr1^{gfp/+}$;CD45.1 donor mice and purified $CD115^+CX_3CR1/GFP^+Gr1^{high}$ monocytes using a high-speed cell sorter (Fig. 7*A*). Purified cells were then

adoptively transferred to *CD11c*:DTR CD45.2 recipients, which were divided into two groups that were treated with DTx on different time points.

One group of recipient mice was treated with DTx i.t. on the day of BM monocyte transfer and analyzed 4 days later (Fig. 7, *B* and *C*). Confirming the results we had obtained with the $Gr1^{high}$ blood monocyte grafts (Fig. 6*C*), we readily observed graft-derived DC in the recipients' lungs, but failed to detect graft-derived MΦ (Fig. 7*B*).

A second group of mice was treated with toxin only 4 days after receiving $Gr1^{+}$ BM monocyte graft. At that time, the majority of graft-derived circulating blood monocytes had converted into $Gr1^{low}$ cells (Fig. 7*C*). Interestingly, the analysis of these recipient mice 4 days after DTx treatment (day 8) revealed the presence of both graft-derived DC and MΦ in their lungs (Fig. 7*D*).

Cumulatively, these results suggest that $Gr1^{high}$ monocytes lack the immediate potential to give rise to lung MΦ, but can gain this function upon conversion into $Gr1^{low}$ monocytes.

Discussion

In this study, we used adoptively transferred blood monocytes to investigate the precursor/progeny relationship between these circulating leukocytes and pulmonary mononuclear phagocytes, including DC and MΦ. Specifically, we studied the differentiation potential of two recently described murine monocyte subsets that can be differentiated according to expression of the Gr1 surface marker.

To study the differentiation potential of monocytes into lung mononuclear phagocytes, we made use of *CD11c*:DTR transgenic mice, which provided us with a tool to specifically ablate pulmonary $CD11c^{+}$ cells, without effecting undifferentiated monocytes (24, 34) (Fig. 3). Depletion of $CD11c^{+}$ cells, including MΦ and DC, promotes the seeding of the pulmonary mononuclear phagocyte system by blood-derived cells (L. Landsman and S. Jung, manuscript in preparation). Importantly, as opposed to other systems (41), our DTx-based depletion strategy is dependent on the genetic background of the mice (24), and non-DTR transgenic donor cells are therefore resistant to ablation upon differentiation into $CD11c^{+}$ cells. However, we cannot exclude that depletion of lung MΦ impairs lung homeostasis and as such provides proinflammatory conditions.

In agreement with studies on the rat intestinal LNs (17), we show that murine monocytes can give rise to lung DC in steady state (Fig. 2). Furthermore, we demonstrate differentiation of blood monocytes into lung DC under inflammation (Fig. 6), thus extending previous reports for skin and peritoneum (7–9). In addition, these monocyte-derived lung DC were capable of reconstituting $CD4^{+}$ T cell priming in an immunodeficient mouse model (Fig. 5). Importantly, we were able to show that both $Gr1^{high}CX_3CR1^{int}$ and $Gr1^{low}CX_3CR1^{high}$ blood monocyte subsets had the potential to give rise to lung DC under both inflammatory and noninflammatory conditions (Fig. 6).

Tissue MΦ are believed to arise from blood monocytes (1). However, direct proof for this connection is largely limited to serosal MΦ in the peritoneal cavity (5). In this study, we provide direct evidence that blood monocytes can give rise to parenchymal lung MΦ in MΦ-depleted recipients and under inflammation (Figs. 4 and 5). However, interestingly, the potential to become a lung MΦ is restricted to the $Gr1^{low}CX_3CR1^{high}$ monocyte subset.

Our results suggest that $Gr1^{high}CX_3CR1^{int}$ and $Gr1^{low}CX_3CR1^{high}$ monocyte subsets respond in the lung differently to the same environmental signal, indicating their commitment to acquire either DC or MΦ fate. Thus, the potential to give rise to lung MΦ was restricted to the $Gr1^{low}$ monocyte subset, whereas $Gr1^{high}$ monocytes seem destined to become lung DC. The latter can, however, gain the potential to become lung MΦ by conversion into $Gr1^{low}$ monocytes (Figs. 6 and 7). Upon differentiation into $Gr1^{low}CCR2^{-}$ cells, $Gr1^{high}CCR2^{+}$ monocytes are likely to lose their ability to respond to inflammatory signals, such as MCP-1 (CCL2) (16, 42). This scenario may reflect the need for DC during inflammation, in which $Gr1^{high}$ monocytes migrate to site of challenge and exclusively give rise to DC. It may ensure limitation of competition on precursor cells by steady-state tasks, such as the generation of tissue MΦ. Replenishment of the lung MΦ population under inflammation might be accomplished by proliferative expansion of local precursors in addition to monocyte differentiation (L. Landsman and S. Jung, manuscript in preparation).

Lung DC and MΦ play opposing roles in the initiation and maintenance of lung inflammations. Whereas DC activate T cells and thereby promote inflammation, pulmonary MΦ suppress these processes (20, 21, 37, 43). It has therefore been suggested that the balance of these two cell types influences the progression of lung inflammation, such as asthma (44, 45). The results presented in this study highlight the differential origins of MΦ and DC in the lung. Although lung DC can develop from both $Gr1^{high}CX_3CR1^{int}$ and $Gr1^{low}CX_3CR1^{high}$ monocyte subsets, lung MΦ originate from $Gr1^{low}$ monocytes. In-depth understanding of the origin of lung DC and MΦ might be of value for the development of cell therapies for respiratory disorders.

Acknowledgments

We thank our laboratory members for critical reading of the manuscript, and are grateful to Y. Chermesh and Y. Melamed for animal husbandry.

Disclosures

The authors have no financial conflict of interest.

References

1. Van Furth, R., and Z. A. Cohn. 1968. The origin and kinetics of mononuclear phagocytes. *J. Exp. Med.* 128: 415–435.
2. Gordon, S., and P. R. Taylor. 2005. Monocyte and macrophage heterogeneity. *Nat. Rev. Immunol.* 5: 953–964.
3. Sallusto, F., and A. Lanzavecchia. 1994. Efficient presentation of soluble antigen by cultured human dendritic cells is maintained by granulocyte/macrophage colony-stimulating factor plus interleukin 4 and down-regulated by tumor necrosis factor α. *J. Exp. Med.* 179: 1109–1118.
4. Wiktor-Jedrzejczak, W., and S. Gordon. 1996. Cytokine regulation of the macrophage (Mϕ) system studied using the colony stimulating factor-1-deficient *op/op* mouse. *Physiol. Rev.* 76: 927–947.
5. Van Furth, R., M. C. Diesselhoff-den Dulk, and H. Mattie. 1973. Quantitative study on the production and kinetics of mononuclear phagocytes during an acute inflammatory reaction. *J. Exp. Med.* 138: 1314–1330.
6. Naito, M., S. Umeda, T. Yamamoto, H. Moriyama, H. Umezu, G. Hasegawa, H. Usuda, L. D. Shultz, and K. Takahashi. 1996. Development, differentiation, and phenotypic heterogeneity of murine tissue macrophages. *J. Leukocyte Biol.* 59: 133–138.
7. Randolph, G. J. 1999. Differentiation of phagocytic monocytes into lymph node dendritic cells in vivo. *Immunity* 11: 753–761.
8. Geissmann, F., S. Jung, and D. R. Littman. 2003. Blood monocytes consist of two principal subsets with distinct migratory properties. *Immunity* 19: 71–82.
9. Ginhoux, F., F. Tacke, V. Angeli, M. Bogunovic, M. Loubeau, X. M. Dai, E. R. Stanley, G. J. Randolph, and M. Merad. 2006. Langerhans cells arise from monocytes in vivo. *Nat. Immunol.* 7: 265–273.
10. Fogg, D. K., C. Sibon, C. Miled, S. Jung, P. Aucouturier, D. R. Littman, A. Cumano, and F. Geissmann. 2006. A clonogenic bone marrow progenitor specific for macrophages and dendritic cells. *Science* 311: 83–87.
11. Naik, S. H., D. Metcalf, A. van Nieuwenhuijze, I. Wicks, L. Wu, M. O'Keeffe, and K. Shortman. 2006. Intrasplenic steady-state dendritic cell precursors that are distinct from monocytes. *Nat. Immunol.* 7: 663–671.
12. Varol, C., L. Landsman, D. K. Fogg, L. Greenshtein, B. Gildor, R. Margalit, V. Kalchenko, F. Geissmann, and S. Jung. 2006. Monocytes give rise to mucosal, but not splenic conventional dendritic cells. *J. Exp. Med.* In press.
13. Passlick, B., D. Flieger, and H. W. Ziegler-Heitbrock. 1989. Identification and characterization of a novel monocyte subpopulation in human peripheral blood. *Blood* 74: 2527–2534.
14. Grage-Griebenow, E., H. D. Flad, and M. Ernst. 2001. Heterogeneity of human peripheral blood monocyte subsets. *J. Leukocyte Biol.* 69: 11–20.
15. Belge, K. U., F. Dayyani, A. Horelt, M. Siedlar, M. Frankenberger, B. Frankenberger, T. Espevik, and L. Ziegler-Heitbrock. 2002. The proinflammatory $CD14^{+}$ $CD16^{+}DR^{++}$ monocytes are a major source of TNF. *J. Immunol.* 168: 3536–3542.

16. Palframan, R. T., S. Jung, G. Cheng, W. Weninger, Y. Luo, M. Dorf, D. R. Littman, B. J. Rollins, H. Zweerink, A. Rot, and U. H. von Andrian. 2001. Inflammatory chemokine transport and presentation in HEV: a remote control mechanism for monocyte recruitment to lymph nodes in inflamed tissues. *J. Exp. Med.* 194: 1361–1373.
17. Yrlid, U., C. D. Jenkins, and G. G. Macpherson. 2006. Relationships between distinct blood monocyte subsets and migrating intestinal lymph dendritic cells in vivo under steady-state conditions. *J. Immunol.* 176: 4155–4162.
18. Sunderkotter, C., T. Nikolic, M. J. Dillon, N. Van Rooijen, M. Stehling, D. A. Drevets, and P. J. Leenen. 2004. Subpopulations of mouse blood monocytes differ in maturation stage and inflammatory response. *J. Immunol.* 172: 4410–4417.
19. Qu, C., E. W. Edwards, F. Tacke, V. Angeli, J. Llodra, G. Sanchez-Schmitz, A. Garin, N. S. Haque, W. Peters, N. van Rooijen, et al. 2004. Role of CCR8 and other chemokine pathways in the migration of monocyte-derived dendritic cells to lymph nodes. *J. Exp. Med.* 200: 1231–1241.
20. Holt, P. G., J. Oliver, N. Bilyk, P. G. McMenamin, G. Kraal, and T. Thepen. 1993. Down-regulation of the antigen presenting cell function(s) of pulmonary dendritic cells in vivo by resident alveolar macrophages. *J. Exp. Med.* 177: 397–407.
21. Julia, V., E. M. Hessel, L. Malherbe, N. Glaichenhaus, A. O'Garra, and R. L. Coffman. 2002. A restricted subset of dendritic cells captures airborne antigens and remains able to activate specific T cells long after antigen exposure. *Immunity* 16: 271–283.
22. Lambrecht, B. N., B. Salomon, D. Klatzmann, and R. A. Pauwels. 1998. Dendritic cells are required for the development of chronic eosinophilic airway inflammation in response to inhaled antigen in sensitized mice. *J. Immunol.* 160: 4090–4097.
23. Gonzalez-Juarrero, M., T. S. Shim, A. Kipnis, A. P. Junqueira-Kipnis, and I. M. Orme. 2003. Dynamics of macrophage cell populations during murine pulmonary tuberculosis. *J. Immunol.* 171: 3128–3135.
24. Jung, S., D. Unutmaz, P. Wong, G. Sano, K. De los Santos, T. Sparwasser, S. Wu, S. Vuthoori, K. Ko, F. Zavala, et al. 2002. In vivo depletion of $CD11c^+$ dendritic cells abrogates priming of $CD8^+$ T cells by exogenous cell-associated antigens. *Immunity* 17: 211–220.
25. Jung, S., J. Aliberti, P. Graemmel, M. J. Sunshine, G. W. Kreutzberg, A. Sher, and D. R. Littman. 2000. Analysis of fractalkine receptor CX_3CR1 function by targeted deletion and green fluorescent protein reporter gene insertion. *Mol. Cell. Biol.* 20: 4106–4114.
26. Borriello, F., M. P. Sethna, S. D. Boyd, A. N. Schweitzer, E. A. Tivol, D. Jacoby, T. B. Strom, E. M. Simpson, G. J. Freeman, and A. H. Sharpe. 1997. B7-1 and B7-2 have overlapping, critical roles in immunoglobulin class switching and germinal center formation. *Immunity* 6: 303–313.
27. Barnden, M. J., J. Allison, W. R. Heath, and F. R. Carbone. 1998. Defective TCR expression in transgenic mice constructed using cDNA-based α- and β-chain genes under the control of heterologous regulatory elements. *Immunol. Cell Biol.* 76: 34–40.
28. Robertson, J. M., P. E. Jensen, and B. D. Evavold. 2000. DO11.10 and OT-II T cells recognize a C-terminal ovalbumin 323–339 epitope. *J. Immunol.* 164: 4706–4712.
29. Ho, W., and A. Furst. 1973. Intratracheal instillation method for mouse lungs. *Oncology* 27: 385–393.
30. Bergner, A., and M. J. Sanderson. 2003. Airway contractility and smooth muscle Ca^{2+} signaling in lung slices from different mouse strains. *J. Appl. Physiol.* 95: 1325–1332.
31. Vermaelen, K., and R. Pauwels. 2004. Accurate and simple discrimination of mouse pulmonary dendritic cell and macrophage populations by flow cytometry: methodology and new insights. *Cytometry A* 61: 170–177.
32. Havenith, C. E., A. J. Breedijk, P. P. van Miert, N. Blijleven, W. Calame, R. H. Beelen, and E. C. Hoefsmit. 1993. Separation of alveolar macrophages and dendritic cells via autofluorescence: phenotypical and functional characterization. *J. Leukocyte Biol.* 53: 504–510.
33. Vallon-Eberhard, A., L. Landsman, N. Yogev, B. Verrier, and S. Jung. 2006. Transepithelial pathogen uptake into the small intestinal lamina propria. *J. Immunol.* 176: 2465–2469.
34. Van Rijt, L. S., S. Jung, A. Kleinjan, N. Vos, M. Willart, C. Duez, H. C. Hoogsteden, and B. N. Lambrecht. 2005. In vivo depletion of lung $CD11c^+$ dendritic cells during allergen challenge abrogates the characteristic features of asthma. *J. Exp. Med.* 201: 981–991.
35. Steinman, R. M., and Z. A. Cohn. 1974. Identification of a novel cell type in peripheral lymphoid organs of mice. II. Functional properties in vitro. *J. Exp. Med.* 139: 380–397.
36. Steinman, R. M. 1999. Dendritic cells. In *Fundamental Immunology*, Vol. 1. W. E. Paul, ed. Lippincott-Raven, Philadelphia, pp. 547–573.
37. Pollard, A. M., and M. F. Lipscomb. 1990. Characterization of murine lung dendritic cells: similarities to Langerhans cells and thymic dendritic cells. *J. Exp. Med.* 172: 159–167.
38. Sharpe, A. H., and G. J. Freeman. 2002. The B7-CD28 superfamily. *Nat. Rev. Immunol.* 2: 116–126.
39. Maus, U. A., S. Janzen, G. Wall, M. Srivastava, T. S. Blackwell, J. W. Christman, W. Seeger, T. Welte, and J. Lohmeyer. 2006. Resident alveolar macrophages are replaced by recruited monocytes in response to endotoxin-induced lung inflammation. *Am. J. Respir. Cell Mol. Biol.* 35: 227–235.
40. Bennett, C. L., E. van Rijn, S. Jung, K. Inaba, R. M. Steinman, M. L. Kapsenberg, and B. E. Clausen. 2005. Inducible ablation of mouse Langerhans cells diminishes but fails to abrogate contact hypersensitivity. *J. Cell Biol.* 169: 569–576.
41. Van Rooijen, N. 1989. The liposome-mediated macrophage 'suicide' technique. *J. Immunol. Methods* 124: 1–6.
42. Maus, U., K. von Grote, W. A. Kuziel, M. Mack, E. J. Miller, J. Cihak, M. Stangassinger, R. Maus, D. Schlondorff, W. Seeger, and J. Lohmeyer. 2002. The role of CC chemokine receptor 2 in alveolar monocyte and neutrophil immigration in intact mice. *Am. J. Respir. Crit. Care Med.* 166: 268–273.
43. Careau, E., and E. Y. Bissonnette. 2004. Adoptive transfer of alveolar macrophages abrogates bronchial hyperresponsiveness. *Am. J. Respir. Cell Mol. Biol.* 31: 22–27.
44. Lambrecht, B. N., and H. Hammad. 2003. Taking our breath away: dendritic cells in the pathogenesis of asthma. *Nat. Rev. Immunol.* 3: 994–1003.
45. Peters-Golden, M. 2004. The alveolar macrophage: the forgotten cell in asthma. *Am. J. Respir. Cell Mol. Biol.* 31: 3–7.